Structure in Solution of the RNA·DNA Hybrid $(rA)_8$·$(dT)_8$ Determined by NMR and Raman Spectroscopy†

Masato Katahira,‡ Sang Jong Lee,‡ Yuji Kobayashi,‡ Hiromu Sugeta,‡ Yoshimasa Kyogoku,‡ Shigenori Iwai,§ Eiko Ohtsuka,§ James M. Benevides,⊥ and George J. Thomas, Jr.*,⊥

Contribution from the Institute for Protein Research, Osaka University, Suita, Osaka 565, Japan, Faculty of Pharmaceutical Sciences, Hokkaido University, Sapporo 060, Japan, and Division of Cell Biology and Biophysics, School of Basic Life Sciences, University of Missouri—Kansas City, Kansas City, Missouri 64110-2499. *Received September 22, 1989*

Abstract: The solution structure of the hybrid RNA·DNA octamer $(rA)_8$·$(dT)_8$ has been determined by nuclear magnetic resonance and laser Raman spectroscopy. The nuclear Overhauser effects resulting from irradiation of thymidine imino protons indicate a duplex structure with conventional Watson–Crick base pairs. The combined results from NMR and Raman spectra are consistent with different nucleotide backbone geometries in $(rA)_8$ and $(dT)_8$ strands. Nucleotide residues of the riboadenylate strand exhibit C3′ endo sugar pucker and phosphodiester conformation similar to that of aqueous RNA (the so-called "A-form" geometry), while residues of the thymidylate strand exhibit C2′ endo sugar pucker and phosphodiester conformation similar to that of aqueous DNA ("B-form" geometry). The solution structure of the hybrid octamer is therefore similar to that proposed previously for poly(rA)·poly(dT) on the basis of fiber X-ray diffraction[1] and solution spectroscopic studies.[2-6] In the model developed here for $(rA)_8$·$(dT)_8$, the distance between the C8–H proton and the phosphoester O5′ atom of each adenylate residue is 2.2 Å, which is sufficient for an intranucleotide C8–H···O5′ hydrogen bond. The presence of intranucleotide C8–H···O5′ hydrogen bonds in $(rA)_n$·$(dT)_n$ solution structures would explain the previously reported resistance of adenine C8–H protons of poly(rA)·poly(dT) to deuterium isotope exchange in D_2O solution.[5]

Fiber X-ray diffraction and ^{31}P NMR studies of poly(rA)·poly(dT) provide evidence of an unusual secondary structure for the hybrid nucleic acid at conditions of high relative humidity.[1,2] The fiber X-ray diffraction pattern was found to be consistent with a model containing C3′ endo ribosyl ring pucker for rA, and C3′ exo deoxyribosyl ring pucker (similar to C2′ endo pucker) for dT, i.e., an A-like conformation in the rA strand and a B-like conformation in the dT strand. This conclusion has been reinforced by Raman spectroscopy of poly(rA)·poly(dT) in independently published work of Thomas et al.[3] and Katahira et al.[4] The Raman spectra also show that the different sugar puckers of rA and dT in the fibers are maintained for poly(rA)·poly(dT) in aqueous solution.

The absence of a B-like conformation for the rA strand of aqueous poly(rA)·poly(dT) is further supported by hydrogen isotope exchange studies, which reveal extraordinary retardation of deuterium exchange of the adenine C8–H group. The kinetics of adenine C8–H exchange in poly(rA)·poly(dT) is several orders of magnitude slower than that observed in the mononucleotide.[5] Such extraordinary retardation of purine C8–H exchange does not occur for B-DNA secondary structures, which typically exhibit 2-fold retardation vis-à-vis mononucleotides; nor does it occur for duplex A RNA secondary structures, which exhibit 8-fold retardation. However, retardation factors greater than several hundred-fold do occur for secondary structures in which solvent access to the purine N7–C8 locus is severely restricted.[6] For example, retardation is greater than 200-fold for multistranded structures in which the third or fourth strand donates hydrogen bonds to purine N7 acceptors, through Hoogsteen base pairing. In apparent contradiction to the X-ray,[1] ^{31}P NMR,[2] Raman,[3-5] and isotope-exchange studies,[6] Gupta and co-workers[7] have interpreted NMR–NOE spectra of aqueous poly(rA)·poly(dT) as evidence for a uniform B-like structure in both the rA and dT strands and have argued specifically against the occurrence of C3′ endo pucker of rA in the solution structure of this RNA·DNA hybrid.

In order to provide a definitive resolution of the $(rA)_n$·$(dT)_n$ solution structure, and to gain additional insight into the structural

† This is part 36 in the series Raman Spectral Studies of Nucleic Acids from the U.S. laboratory and is supported by grants from the U.S. NIH (AI18758) and NSF (U.S-Japan INT83-11189).

‡ Osaka University.
§ Hokkaido University.
⊥ University of Missouri—Kansas City.

(1) Zimmerman, S. B.; Pheiffer, B. H. *Proc. Natl. Acad. Sci. U.S.A.* **1981**, *78*, 78–82.
(2) Shindo, H.; Matsumoto, U. *J. Biol. Chem.* **1984**, *259*, 8682–8684.
(3) Thomas, G. J., Jr.; Benevides, J. M.; Prescott, B. *Biomolecular Stereodynamics*; **1986**; Vol. IV, pp 227–253, (Proceedings of the Fourth Conversation in the Discipline Biomolecular Stereodynamics, June 4–8, 1985, SUNY—Albany).
(4) Katahira, M.; Nishimura, Y.; Tsuboi, M.; Sato, T.; Mitsui, Y.; Iitaka, Y. *Biochim. Biophys. Acta* **1986**, *867*, 256–267.
(5) Benevides, J. M.; Thomas, G. J., Jr. *Biochemistry* **1988**, *27*, 3868–3873.
(6) Benevides, J. M.; Thomas, G. J., Jr. *Biopolymers* **1985**, *24*, 667–682.
(7) Gupta, G.; Sarma, M. H.; Sarma, R. H. *J. Mol. Biol.* **1985**, *186*, 463–469.
(8) Clore, G. M.; Kimber, B. J.; Gronenborn, A. M. *J. Magn. Reson.* **1983**, *54*, 170–173.
(9) Nishimura, Y.; Tsuboi, M.; Nakano, T.; Higuchi, S.; Sato, T.; Shida, T.; Uesugi, S.; Ohtsuka, E.; Ikehara, M. *Nucleic Acids Res.* **1983**, *11*, 1579–1588.
(10) Nishimura, Y.; Torigoe, C.; Tsuboi, M. *Nucleic Acids Res.* **1986**, *14*, 2737–2748.
(11) Benevides, J. M.; Wang, A. H.-J.; van der Marel, G. A.; van Boom, J. H.; Rich, A.; Thomas, G. J., Jr. *Nucleic Acids Res.* **1984**, *12*, 5913–5925. Thomas, G. J., Jr.; Benevides, J. M. *Biopolymers* **1985**, *24*, 1101–1104.
(12) Benevides, J. M.; Wang, A. H.-J; Rich, A.; Kyogoku, Y.; van der Marel, G. A.; van Boom, J. H.; Thomas, G. J., Jr. *Biochemistry* **1986**, *25*, 41–50.
(13) Benevides, J. M.; Wang, A. H.-J.; van der Marel, G. A.; van Boom, J. H.; Thomas, G. J., Jr. *Biochemistry* **1988**, *27*, 931–938.
(14) Erfurth, S. C.; Kiser, E. J.; Peticolas, W. L. *Proc. Natl. Acad. Sci. U.S.A.* **1972**, *69*, 938–941. Erfurth, S. C.; Bond, P. J.; Peticolas, W. L. *Biopolymers* **1975**, *14*, 1245–1257.
(15) Torigoe, C.; Nishimura, Y.; Tsuboi, M.; Matsuzaki, J.; Hotoda, H.; Sekine, M.; Hata, T. *Spectrochim. Acta* **1986**, *42A*, 1101–1106.
(16) Nishimura, Y.; Torigoe, C.; Katahira, M.; Tate, S.; Tanaka, K.; Tsuboi, M.; Matsuzaki, J.; Hotoda, H.; Sekine, M.; Hata, T. *Nucleic Acids Symp. Ser.* **1986**, *No. 17*, 195–198.
(17) Thomas, G. A.; Peticolas, W. L. *J. Am. Chem. Soc.* **1983**, *105*, 993–996.
(18) Arnott, S.; Chandrasekaran, R.; Hall, I. H.; Puigjaner, L. C. *Nucleic Acids Res.* **1983**, *11*, 4141–4155.
(19) Arnott, S.; Hukins, D. W. *Biochem. Biophys. Res. Commun.* **1972**, *47*, 1504–1509.
(20) Arnott, S.; Selsing, E. *J. Mol. Biol.* **1974**, *88*, 509–521.
(21) Chandrasekaran, R.; Arnott, S. In *Biophysics*; Saenger, W., Ed.; Springer-Verlag: New York, 1989.
(22) Arnott, S.; Chandrasekaran, R.; Millane, R. P.; Park, H.-S. *J. Mol. Biol.* **1986**, *188*, 631–640.

0002-7863/90/1512-4508$02.50/0

basis for the extraordinary retardation of adenine C8–H exchange in the polymer, we have examined both the NMR spectra and the Raman spectra of the hybrid octamer $(rA)_8$·$(dT)_8$. This octanucelotide analogue of poly(rA)·poly(dT) offers advantages for NMR spectroscopy of narrower line width and improved resolution to assess the conformational features in detail. Nucleoside sugar pucker and phosphodiester geometry of the octamer duplex can also be conveniently categorized by Raman spectroscopy. Apart from possible end effects, the conformation of $(rA)_8$·$(dT)_8$ is expected to be the same as that of the corresponding polynucleotide. The present results are of interest both for the importance of hybrid RNA·DNA structures as models for transcription and replication and for the possible contribution of hydrogen-bonding interactions at the purine N7–C8 locus toward stabilization of hybrid nucleic acid structures in solution.

The present results are relevant to the hydrogen isotope exchange properties of (rA)·(dT) structures in particular and may also be relevant to other ribosylpurine–deoxyribosylpyrimidine complexes. The extraordinarily slow deuterium exchange of C8–H groups observed for rA residues of poly(rA)·poly(dT) has suggested an unusual intranucleotide hydrogen bond involving the adenine C8–H group as donor.[5] The NOE difference spectra resulting from irradiation of thymidine imino protons demonstrate Watson–Crick base pairing in $(rA)_8$·$(dT)_8$ and rule out unconventional base pairs of the Hoogsteen type. The present results therefore provide indirect confirmation of the proposed C8–H donor interaction as the source of retardation of C8–H exchange.

Materials and Methods

The octa(ribo)nucleotide $(rA)_8$ synthesized as reported elsewhere,[35] and the octa(deoxyribo)nucleotide $(dT)_8$ purchased from Pharmacia, were dissolved in 0.01 M NaCl at pH 7 and mixed in equimolar ratio by using known extinction coefficients of poly(rA) and poly(dT). The complex was lyophilized and stored for subsequent use. For the measurement of Raman spectra, lyophilized samples were dissolved to a concentration in the range 5–15 mM in 0.1 M NaCl solution (pH 7) and sealed in glass capillaries. Raman spectra were recorded at laboratories both in Japan (Institute for Protein Research) and the United States (Southeastern Massachusetts University and University of Missouri—Kansas City). In the Japan laboratory, the spectra were excited by using approximately 300 mW of 514.5-nm radiation from a Spectra-Physics 164 Ar^+ laser and the data were collected on a JEOL JRS-400D spectrophotometer, interfaced with a NEC PC-9800 personal computer for data processing. In the U.S. laboratories, 300 mW of 514.5-nm excitation was provided by a Coherent Innova-70 Ar^+ laser and the spectra were collected on a Spex Ramalog spectrometer under the control of a North Star Horizon-II microcomputer.

We measured the temperature dependence of the ultraviolet absorption (UV) spectra of $(rA)_8$·$(dT)_8$ in the same buffers employed for NMR and Raman measurements. The results indicated a median melting temperature (T_m) above 10 °C, at the solute concentration of 0.05 mM employed for UV spectroscopy. A somewhat higher T_m is expected at the higher solute concentrations employed for NMR and Raman spectroscopy. Indeed, we observed imino proton peaks by NMR, which assured base pairing at 15 °C for 3.5 mM solutions. Raman bands characteristic of an ordered backbone were also evident at 20 °C for 10 mM solutions. Nonetheless, to ensure complete formation of the duplex, all of the experiments described below were carried out below 15 °C. Because of the relatively low T_m of $(rA)_8$·$(dT)_8$, it was not feasible to conduct deuterium-exchange studies directly on the octamer complex.

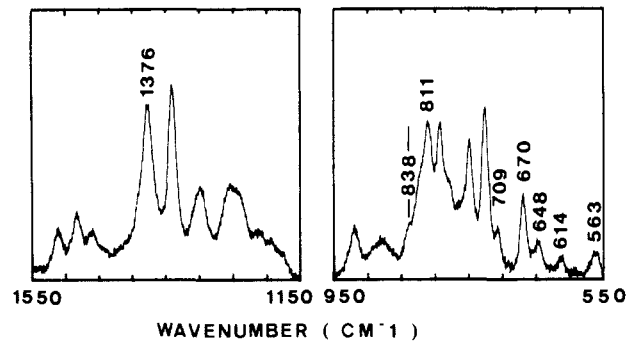

Figure 1. Raman spectrum in the regions 550–950 and 1150–1550 cm^{-1} of $(rA)_8$·$(dT)_8$ in H_2O solution at pH 7 and 2 °C.

For the measurement of NMR spectra of nonexchangeable protons, lyophilized samples were dissolved in a solution containing 0.1 M NaCl and 10 mM phosphate buffer at pH 7.0. The solution was again lyophilized and the duplex was redissolved to a concentration of 3.5 mM in pure (99.96%) D_2O. For the measurement of exchangeable proton spectra, a 9:1 mixture of H_2O–D_2O was substituted for the pure D_2O. DSS was used as an internal chemical shift reference.

NMR spectra were obtained with a JEOL GX-500 NMR spectrometer. Spectra in H_2O were accumulated with a 1-1 pulse sequence,[8] and NOE difference spectra were obtained by difference FID between on and off resonance irradiation at 5 °C. Irradiation time was 100 ms. Phase-sensitive NOESY and DQF-COSY[36] spectra in D_2O were collected by the method of States et al.[37] at 5 and 15 °C. The repetition delay was 2.2 s. Two mixing times, 60 and 100 ms, were used for the NOESY experiments.

Before the measurement of both Raman and NMR spectra, solutions of $(rA)_8$·$(dT)_8$ were heated to 50 °C and cooled gradually to completely anneal the complementary strands. All glassware was cleaned in detergent solutions or heated before use to inactivate possible traces of nucleases.

Results

NMR spectroscopy of $(rA)_8$·$(dT)_8$ in 3.5 mM solution reveals imino proton peaks, which assure base pairing up to 15 °C. Therefore, the following studies of $(rA)_8$·$(dT)_8$ in 10 mM solution at 2 °C by Raman spectroscopy, and at 5 and 15 °C by NMR spectroscopy, reflect the structure of the $(rA)_8$·$(dT)_8$ duplex.

1. Raman Spectroscopy. The Raman spectra of $(rA)_8$·$(dT)_8$ in the regions 550–950 and 1150–1550 cm^{-1} are shown in Figure 1. Many of the Raman bands in the spectra of Figure 1 serve as indicators of nucleoside sugar pucker and backbone phosphodiester conformation. The use of Raman bands as indicators of nucleoside and phosphodiester conformations rests upon correlations established previously in Raman studies of DNA and RNA crystals of known structure,[3,4,9-13] and of polynucleotide fibers of known configuration.[3,4,10,14-17] Applying the established correlations to $(rA)_8$·$(dT)_8$, in the same manner as in their analogous application to poly(rA)·poly(dT),[3-5] we find that the frequencies and intensities of the Raman peaks at 811 and 838 cm^{-1} identify a 1:1 ratio of A-form and B-form phosphodiester geometries in the hybrid octamer. Further, the weak Raman lines at 563 and 614 cm^{-1}, and the more intense lines at 670 and 1376 cm^{-1}, indicate that thymidine residues of $(rA)_8$·$(dT)_8$ exist only with C2′ endo sugar pucker, consistent with phosphodiester geometry of the B form in the $(dT)_8$ strand.[6] Finally, the band at 648 cm^{-1} is a recognized marker for the C3′ endo conformer of the adenosine residue, consistent with phosphodiester geometry of the A form

(23) Wüthrich, K. *NMR of Proteins and Nucleic Acids*; John Wiley and Sons, Inc.: New York, 1986.
(24) Chou, S. H.; Flynn, P.; Reid, B. *Biochemistry* **1989**, *28*, 2422–2435.
(25) Chou, S. H.; Flynn, P.; Reid, B. *Biochemistry* **1989**, *28*, 2435–2443.
(26) Reid, D. G.; Salisbury, S. A.; Bellard, S.; Shakked, A.; Williams, D. H. *Biochemistry* **1983**, *22*, 2019–2025.
(27) Clore, M.; Gronenborn, A. M.; McLaughlin, L. W. *Eur. J. Biochem.* **1985**, *151*, 153–165.
(28) Mellema, J. R.; Haasnoot, C. A. A.; van der Marel, G. A.; Wille, G.; van Boeckel, C. A. A.; van Boom, J. H.; Altona, C. *Nucleic Acids Res.* **1983**, *11*, 5717–5738.
(29) Behling, R. W.; Kearns, D. R. *Biochemistry* **1986**, *25*, 3335–3346.
(30) Kintanar, A.; Klevit, R. E.; Reid, B. *Nucleic Acids Res.* **1987**, *15*, 5845–5862.
(31) (a) Katahira, M.; Sugeta, H.; Kyogoku, Y.; Fujii, S.; Fujisawa, R.; Tomita, K. *Nucleic Acids Res.* **1988**, *16*, 8619–8632. (b) Katahira, M.; Hiromu, S.; Kyogoku, Y. *Nucleic Acids Res.* **1990**, *18*, 613–618. (c) Katahira, M.; Sugeta, H.; Kyogoku, Y.; Fujii, S. *Biochemistry*, in press.
(32) Nadeau, J. G.; Crothers, D. M. *Proc. Natl. Acad. Sci. U.S.A.* **1989**, *86*, 2622–2626.
(33) Celda, B.; Widmer, H.; Leupin, W.; Chazin, W. J.; Denny, W. A.; Wüthrich, K. *Biochemistry* **1989**, *28*, 1462–1471.
(34) Hosur, R. V.; Ravikumar, M.; Chary, K. V. R.; Steth, A.; Govil, G.; Zu-Kun, T.; Miles, H. T. *FEBS Lett.* **1986**, *205*, 71–76.
(35) Iwai, S.; Ohtsuka, E. *Nucleic Acids Res.* **1988**, *16*, 9443–9456.
(36) Jeener, J.; Meier, B. H.; Backman, P.; Ernst, R. R. *J. Chem. Phys.* **1979**, *71*, 4546–4553.
(37) States, D. J.; Haberkorn, R. A.; Ruben, D. J. *J. Magn. Reson.* **1987**, *48*, 286–292.

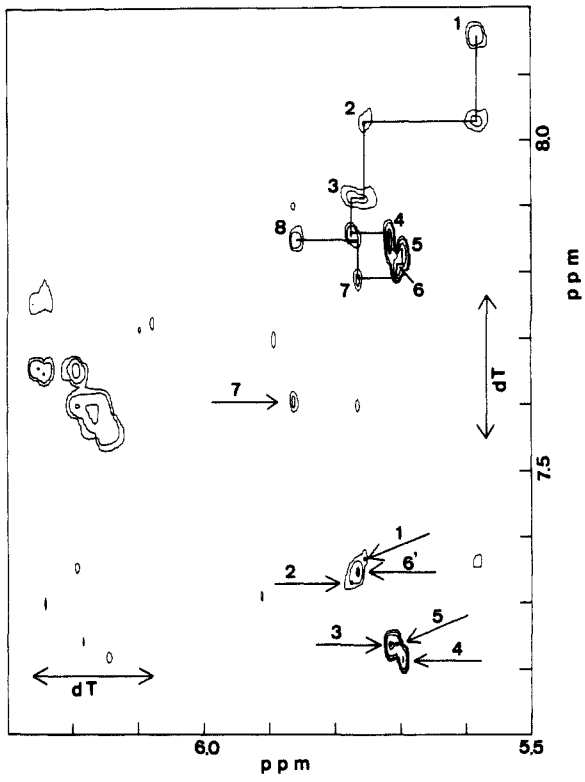

Figure 2. Expansion of the ^{1}H NMR NOESY spectrum of $(rA)_8$·$(dT)_8$ obtained in D_2O buffer at 15 °C and with 100-ms mixing time. Solid lines indicate the H1′(i)/H1′(i − 1)–H8(i) connectivities for the $(rA)_8$ strand, with the H1′(i)–H8(i) cross peaks labeled. Single arrows indicate the H2(i)–H1′(i + 1) cross peaks for the $(rA)_8$ strand and numbering of adenine H2 is denoted. Double arrows indicate the respective ranges where H1′ and H6 resonances of dT residues appear. (See Discussion.)

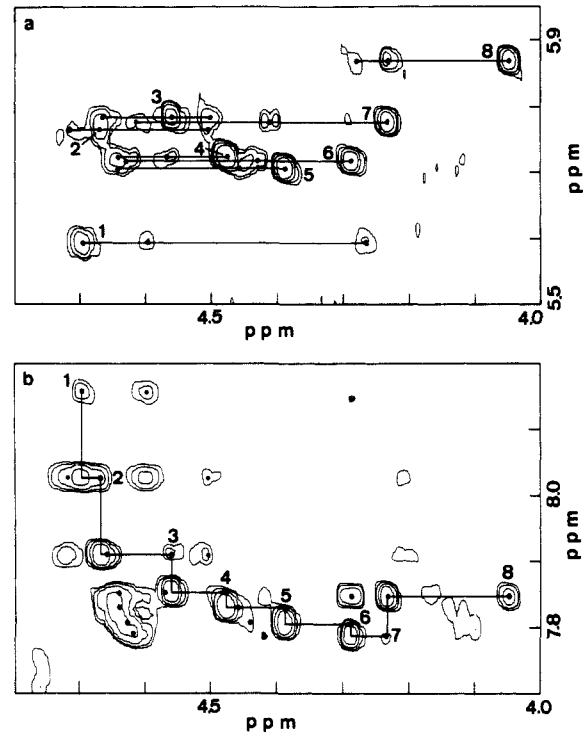

Figure 3. Expansion of the NOESY spectrum, showing cross peaks involving H1′ (top panel, a) and H8 (bottom panel, b), with either H2′ or H3′ or H4′, for each rA residue. In each panel, cross peaks involving H2′ are labeled, and of the two dots remaining unlabeled, the lower field dot is the cross peak involving H3′, while the higher field dot is the cross peak involving H4′ for each residue. (Discrimination of H3′ and H4′ was performed without making any assumptions about relative positions of resonances. See text.) Solid lines in (a) connect intraresidue cross peaks between H2′/H3′/H4′ and H1′. Solid lines in (b) indicate H2′(i)/H2′(i − 1)–H8(i) connectivities for the $(rA)_8$ strand, with H2′(i)–H8(i) cross peaks labeled.

in the $(rA)_8$ strand.[5,6] Therefore, all of the Raman conformation markers of $(rA)_8$·$(dT)_8$, as well as their relative intensities, indicate a 1:1 A:B structure.

The data of Figure 1 are virtually identical with those obtained previously on poly(rA)·poly(dT).[3-5] Accordingly, the structural conclusions reached here for $(rA)_8$·$(dT)_8$ apply also to poly(rA)·poly(dT).

2. NMR Spectroscopy. The numbering of the $(rA)_8$·$(dT)_8$ residues is given in formula I:

	1	2	3	4	5	6	7	8	
5′r	A	A	A	A	A	A	A	A	
	·	·	·	·	·	·	·	·	(I)
3′d	T	T	T	T	T	T	T	T	
	16	15	14	13	12	11	10	9	

The results that follow were obtained from analysis of both the NOESY spectrum with 100 ms mixing time and the DQF-COSY spectrum at 15 °C. The same results were obtained from NOESY and DQF-COSY spectra at 5 °C, where intrinsic conformational features of $(rA)_8$·$(dT)_8$ are reflected more clearly owing to reduced thermal fluctuations, and from the NOESY spectrum with 60-ms mixing time, where the spin diffusion effect is less than that for the 100-ms mixing time.

Assignments of nonexchangeable protons have been accomplished by two-dimensional NMR spectroscopy. Figure 2 shows an expansion of the H1′–H2/H6/H8 cross-peak region in the NOESY spectrum with 100-ms mixing time. Although crowding of resonances of the dT residues renders a complete assignment impracticable, the frequency ranges of the dT resonances can be unambiguously identified. The range for thymine CH_3 is easily recognized, as usual for methyl resonances. The range for H2′/H2″ resonances of dT near 2.5 ppm is established by the fact that H2′ resonances of ribonucleotides (rA) do not appear near 2.5 ppm, but near 4.5 ppm. Accordingly, the ranges for H6 and H1′ of dT residues can be determined as shown in Figure 2, based upon analysis of the apparent cross peaks for H6(i − 1)/H6(i)–CH_3(i), H2′(i)/H2′(i − 1)–H6(i), H2″(i)/H2″(i − 1)–H6(i), H1′(i)–H2′(i), and H1′(i)–H2″(i). Conversely, cross peaks in Figure 3a and b originate only from rA residues. Here, i represents a given base residue as defined in formula I, and conventional notation is employed for sugar and base protons.

In Figure 2, the H1′(i)/H1′(i − 1)–H8(i) connectivities for the rA strand are shown in the upper right of the illustration. Thus, H8 and H1′ resonances of the rA residues can be assigned. Peaks remaining unassigned in the aromatic region of the one-dimensional spectrum and giving no cross peaks to H2′/H3′/H4′ are the H2 resonances of the rA residues. Cross peaks between H2 and H1′ of rA are observed, as denoted in Figure 2 by single arrows (lower right of illustration). Intensities of these cross peaks are not weak, but comparable with intensities of H8(i)–H1′(i) cross peaks. To assist in assigning the cross peaks, we calculated the intra- and interresidue H2–H1′ distances and the H8(i)–H1′(i) distances along the rA strand, assuming each of the following models: (1) B-form structure of Arnott and Hukins,[19] (2) B′-form structure of Arnott and Selsing,[20] (3) A-form structure,[19] (4) hybrid structure of Zimmerman,[1] and (5) hybrid structure of Arnott et al.[18] The calculated interproton distances are listed in the corresponding columns of Table I.

Examination of Table I shows that the H8(i)–H1′(i) distance is between 3.7 and 3.9 Å in all models. Among the three types of H2–H1′ distances [i.e., H2(i)–H1′(i), H2(i)–H1′(i − 1) and H2(i)–H1′(i + 1)], all are significantly greater than 4.0 Å, *except H2(i)–H1′(i + 1) of models 3, 4, and 5.* Accordingly, only for the latter models is a cross peak of intensity comparable to that of H8(i)–H1′(i) expected. Other H2(i)–H1′(i) and H2(i)–H1′(i − 1) distances (Table I) exceed 4.5 Å, and only much weaker cross peaks can be expected from them. Therefore, the cross peaks denoted by single-headed arrows in Figure 2 are attributed with confidence to H2(i)–H1′(i + 1). By use of these cross peaks, H2 resonances of A(1) through A(7) are assigned. Finally, the single

Table I. Intra- and Interresidue Distances (AH2–AH1′ and AH8–AH2′), and Intraresidue Distances (AH8–AH1′) in Selected Models for $(rA)_8$·$(dT)_8$[a]

distance[b]	model[c] 1	2	3	4	5
AH2(i)–AH1′(i)	4.5	4.5	4.7	4.9	4.6
AH2(i)–AH1′($i-1$)	7.2	7.1	8.8	8.6	7.7
AH2(i)–AH1′($i+1$)	4.5	4.4	4.0	3.5	3.3
AH8(i)–AH1′(i)	3.9	3.9	3.8	3.7	3.8
AH8(i)–AH2′(i)	2.2	2.1	3.8	4.2	3.9
AH8(i)–AH2′($i-1$)	3.7	3.8	1.7	1.6	1.9

[a] Distances are in angstroms. Interproton distances were calculated by generating appropriate proton coordinates based upon the carbon coordinates published in the references cited. [b] Three-residue sequences of the rA strand, in the 5′ to 3′ direction, are indicated by $i-1$, i, and $i+1$. [c] Models: 1, B form;[19] 2, B′ form;[20] 3, A form;[19] 4, Zimmerman;[1] 5, Arnott.[18]

peak remaining unassigned in the aromatic region of the one-dimensional spectrum is assigned to H2 of the residue A(8). Assignments of the H2 peaks are also confirmed by A(6)H2–A(7)H2 and A(7)H2–A(8)H2 cross peaks (data not shown).

Horizontal lines in Figure 3a are drawn to connect cross peaks of H1′ to H2′, H3′, and H4′ for each rA residue. The strongest peaks for each rA residue are labeled and assigned as H1′ to H2′ cross peaks, since the distances between them are the shortest for virtually all puckering geometries of the sugar ring.[23,24] (Only for puckering around O4′ endo is the H1′–H4′ distance shorter than H1′–H2′.[23]) We examined the H2′(i)/H2′($i-1$)–H8(i) connectivities to confirm assignments of the H2′ resonances. Cross peaks between previously assigned H8 and tentatively assigned H2′ (on the basis of Figure 3a) can be connected sequentially without contradiction, as shown in Figure 3b. It turns out that very strong interresidue cross peaks appear in these connectivities. Such strong cross peaks are not expected for H4′($i-1$)–H8(i), since the corresponding distances are greater than 4.5 Å in all of the model structures.[23] On the other hand, the H2′($i-1$)–H8(i) distance is much shorter (<2.1 Å) only in the A-form model structure,[19,23] and accordingly, a strong cross peak can be expected. Therefore, misassignment of H4′ as H2′ is improbable and the tentative assignment scheme of H2′ is confirmed. In effect, the assignment of H2′ is accomplished without any assumption a priori about sugar puckering.

The remaining cross peaks, except for H1′–H2′ in Figure 3a, are of intraresidue H1′–H3′ and H1′–H4′ origin and indicate the resonance positions of H3′ and H4′ of the rA residues. These positions are confirmed by H3′(i)–H8(i) and H4′(i)–H8(i) cross peaks, indicated by dots in Figure 3b, by H3′($i-1$)–H8(i) and H4′($i-1$)–H8(i) connectivities, not drawn in Figure 3b, and by H3–H4′ cross peaks (data not shown). Since the H1′–H4′ distance is shorter than H1′–H3′, regardless of sugar puckering,[23] the stronger cross peaks can be attributed to H1–H4′ and the weaker to H1′–H3′. Thus, discrimination between H3′ and H4′ of rA residues is accomplished except for the residues A(3), A(4), and A(6), where discrimination is hindered by overlapping of cross peaks. Examination of H2′–H3′ and H2′–H4′ cross peaks in the NOESY spectrum overcomes the remaining ambiguity. The H2′–H3′ distance (~2.3 Å) is much shorter than H2′–H4′ (3.5–3.9 Å), regardless of sugar puckering,[23] so a stronger cross peak is expected for H2′–H3′, and a weaker one for H2′–H4′. Thus, discrimination of H3′ and H4′ is accomplished for A(3), A(4), and A(6) residues, with further confirmation of the other residue assignments. We note that the position of the H4′ resonance is located at higher field than that of the H3′ resonance for every rA residue (Table II), as is usually the case for a DNA duplex. However, no empirical assumptions were made about the relative positions of H3′ and H4′ resonances in assigning them.

Finally, we note that all of the above assignments have been confirmed by a DQF-COSY spectrum (data not shown).

Discussion

The imino proton resonances of dT residues were observed at either 5 or 15 °C, and NOE difference spectra were obtained by irradiating each imino proton peak. The NOEs to H2 resonances of rA residues were observed on irradiation at each peak (data not shown). These results provide direct evidence that base pairing in $(rA)_8$·$(dT)_8$ is of the conventional Watson–Crick type and not of the Hoogsteen type, where NOEs to H8 or rA residues would be expected.

Table II. Assignments for Nonexchangeable Protons of the rA Strand of $(rA)_8$·$(dT)_8$[a]

residue	H8	H2	H1′	H2′	H3′	H4′
A(1)	8.15	7.36	5.59	4.70	4.60	4.26
A(2)	8.02	7.32	5.76	4.67	4.72	4.50
A(3)	7.91	7.24	5.78	4.56	4.66	4.50
A(4)	7.85	7.21	5.72	4.48	4.64	4.57
A(5)	7.82	7.24	5.70	4.39	4.64	4.46
A(6)	7.81	7.34	5.71	4.28	4.63	4.43
A(7)	7.79	7.60	5.77	4.23	4.62	4.42
A(8)	7.84	7.89	5.86	4.04	4.29	4.23

[a] Excluding H5′ and H5″; chemical shifts (ppm) at 15 °C.

In Figure 3b, H2′($i-1$)–H8(i) cross peaks are uniformly very strong. This is a characteristic typical of the A-form secondary structure with C3′ endo sugar puckering.[23,24,26-28] Weaker H2′(i)–H8(i) cross peaks are also consistent with the A form (Table I).[19,23] It should be stressed that in Figure 3b we can trace sequential H2′(i)/H2′($i-1$)–H8(i) connectivities and observe strong H2′($i-1$)–H8(i) cross peaks and weak H2′(i)–H8(i) cross peaks characteristic of the A-form secondary structure, without any assumption about the conformation of the $(rA)_8$ strand.

As shown in Figure 2, we observe $(rA)_8$ *intra*strand H2–H1′ cross peaks of moderate intensity, nearly comparable to that of H8(i)–H1′(i) cross peaks. As noted above, these peaks are attributed exclusively to H2(i)–H1′($i+1$) cross peaks, because other intrastrand distances are too large to account for them in all of the model structures. A common feature of the A-form,[19] Zimmerman,[1] and Arnott models,[18] where the H2(i)–H1′($i+1$) distance should generate a significant cross peak, is that the adenylate strand (rA or dA) is in the A conformation. Thus, appearance of the moderately intense intrastrand H2–H1′ cross peak not only facilitates assignment of H2 of the rA residues, but also gives information about the strand conformation: The observed cross peaks reveal that the $(rA)_8$ strand is the A conformation in the $(rA)_8$·$(dT)_8$ complex.

The *inter*strand cross peak between H2 of adenine and H1′ of the neighboring 3′-residue of the complementary strand has already been reported for the B form. The intensity of this interstrand cross peak is remarkable in DNA containing the oligo(dA) tract, where it is nearly comparable to the intensity of the H8(i)–H1′(i) cross peak[30,31] and can be used as an indicator of the width of the minor groove.[29-31] However, even in these cases, the intrastrand H2(i)–H1′($i+1$) cross peak is somewhat weaker than the H8(i)–H1′(i) cross peak. Also, in recent reports on DNAs containing the oligo(dA) tract, most of the intrastrand H2(i)–H1′($i+1$) cross peaks are not so intense as to be comparable with the H8(i)–H1′(i) cross peaks. Thus, we suggest here that the intense intrastrand H2(i)–H1′($i+1$) cross peak can be a reliable indicator of the A-form secondary structure. Very recently, Reid and co-workers[24,25] observed similar intense cross peaks for the A conformation.

In the DQF-COSY spectrum, H1′–H2′ cross peaks of rA residues do not appear, with the exception of a very weak one for A(8). On the other hand, H3′–H4′ cross peaks do appear for all rA residues (data not shown). On the basis of a proposed correlation between the H–C–C–H dihedral angle and the corresponding three-bond coupling constant,[34] the sugar puckering is concluded to be C3′ endo, characteristic of the A form, where the H1′–H2′ coupling constant is zero and the corresponding cross peak is not expected to appear. Conversely, the H3′–H4′ coupling constant is ~9 Hz and the corresponding cross peak is expected.

In summary, it is shown by NMR spectroscopy, independently of Raman spectroscopy, that the $(rA)_8$ strand assumes the A-like conformation with C3′ endo sugar puckering. This conclusion rests upon three lines of experimental evidence: (1) very strong

H2′(i − 1)–H8(i) cross peaks in the NOESY spectrum, (2) relatively intense intrastrand H2(i)–H1′(i + 1) cross peaks, comparable with H8(i)–H1′(i) cross peaks in the NOESY spectrum, and (3) absence of H1′–H2′ and presence of H3′–H4′ cross peaks in the DQF-COSY spectrum.

Gupta and co-workers[7] proposed, on the basis of the presumed absence of H3′(i)/H3′(i − 1)–H8(i) NOEs, that the poly(rA) strand of poly(rA)·poly(dT) assumes a B-like conformation. However, Figure 3b shows that H3′(i)–H8(i) cross peaks (labeled with dots) and H3′(i − 1)–H8(i) cross peaks (present, but not explicitly labeled) do occur for $(rA)_8$ in the NOESY spectrum of $(rA)_8$·$(dT)_8$. Except for a few of the cross peaks, band overlap makes it difficult to evaluate the intensities precisely. Yet, it is clear that the intensities are not as weak as would be expected for the B-form structure, where the respective H3′(i)–H8(i) and H3′(i − 1)–H8(i) distances are greater than 5.0 and 4.6 Å.[23] Moreover, as already noted,[25] the absence of H3′(i)/H3′(i − 1)–H8(i) NOEs as criteria for excluding A-form structures is unreliable. Our three independent lines of NMR evidence, summarized in the preceding paragraph, indicate unambiguously that the $(rA)_8$ strand of $(rA)_8$·$(dT)_8$ takes on the A conformation; and this conclusion is further corroborated by Raman spectroscopy (Figure 1).

As mentioned above, complete assignments for dT residues are not feasible because of overlapping of cross peaks. However, some conformational features of the $(dT)_8$ strand can be deduced by NMR spectroscopy. By use of the H2′–H2″ cross-peak region near 2.5 ppm of the NOESY spectrum, where resonances of dT residues only appear, pairing of H2′ and H2″ for each dT residue can be established (data not shown). The range of H1′ resonances of dT residues is limited (Figure 2) and has been discussed above. With this information, discrimination between H2′ and H2″ can be made by comparison of the intensities of H1′–H2′ and H1′–H2″ cross peaks in the NOESY spectrum, since H2″ is closer to H1′ regardless of sugar puckering. Thus, although residue numbering cannot be established, the positions of H2′ and H2″ resonances of dT residues are determined. It then turns out that H1′–H2′ cross peaks, but not H2″–H3′ cross peaks, are observed for six or seven of the dT residues in the DQF-COSY spectrum (data not shown). When the relation between dihedral angle and the corresponding coupling constant is invoked,[34] it is clear that virtually all of the dT sugars (i.e., excluding possible end effects) are restricted to puckering between O4′ and C3′ exo, i.e., within the C2′ endo family. This is consistent with the conclusion from Raman spectroscopy, that dT sugar puckering is not of the C3′ endo family (A form) but of the C2′ endo family (B form).[3-6]

The conformational dissimilarity between $(rA)_8$ and $(dT)_8$ strands may also be reflected in the NOE base–base cross peaks. At least five and possibly six H6(i + 1)–H6(i) cross peaks are observed for the $(dT)_8$ strand, while no H8(i + 1)–H8(i) cross peak is observed for the $(rA)_8$ strand (data not shown). This may result from significantly different intrastrand base stacking in the two strands, although different spin diffusion paths, for example via CH_3 and H2″ in $(dT)_8$ cannot be ruled out. A similar observation has been made recently for another RNA·DNA hybrid.[25] Finally, we note that the interstrand H2–H1′ cross peak is very weak or absent in the NOESY spectrum of $(rA)_8$·$(dT)_8$ (Figure 2), although the relatively intense interstrand cross peak between H2 of adenine and H1′ of the neighboring residue on the complementary strand is observed clearly in the $(dA)_n$·$(dT)_n$ portion of the duplex.[29-33] Again, this is not inconsistent with the results reported recently for another RNA·DNA hybrid,[25] wherein cross peaks are strong only in the direction *from* a C2′ endo strand *to* a C3′ endo strand and very weak or absent otherwise.

A particularly attractive feature of the Zimmerman and Pheiffer model[1] is its kinship to certain geometrical properties of B DNA, despite the C3′ endo puckering of the rA strand. For example, the bases in this model are centered close to the helix axis, as in B DNA, and this is evident from a perspective along the helix axis.[5] In a recent study of poly(rA)·poly(dT), Benevides and Thomas[5] proposed a quite similar model to explain the observed Raman, NMR, and X-ray results on the polynucleotide hybrid. The seemingly conflicting conclusion reached in the earlier NMR study,[7] that poly(rA)·poly(dT) assumes a B conformation, might also be explained by the disposition of the bases close to the helix axis in this structure.

Conclusions

With the combined use of Raman and NMR spectroscopy, the solution conformation of $(rA)_8$·$(dT)_8$ has been determined. The structure is a right-handed double helix and the base pairs are of the Watson–Crick type. No evidence of Hoogsteen or other unusual base pairing is evident in the NMR–NOE spectra. Similarly, no other specific hydrogen-bonding interactions to the adenine N7 acceptor site are apparent.

The conformations of rA and dT strands are inequivalent: *the adenosine residues exhibit C3′ endo sugar pucker; the thymidine residues exhibit sugar pucker in the C2′ endo family.* This conclusion applies rigorously to the central six residues, which are insulated from end effects. The present results are consistent with earlier Raman studies of poly(rA)·poly(dT), which indicated equal amounts of A-type and B-type phosphodiester conformations in the hybrid nucleic acid.[3-5] Among available molecular models, the Zimmerman and Pheiffer model[1] for poly(rA)·poly(dT) is the most consistent with the primary structure and observed NMR, Raman, and isotope-exchange properties of $(rA)_8$·$(dT)_8$.[5] An added attraction of this model is the similarity of its pitch and shape to 10.5-fold B DNA, despite the ribosyl sugars and C3′ endo pucker of residues in the rA strand.

The results obtained here on $(rA)_8$·$(dT)_8$ suggest that the retardation of exchange of adenine C8–H groups in poly(rA)·poly(dT) cannot be explained by Hoogsteen pairing or other hydrogen bonding directly to the N7 purine acceptor and therefore probably result from another specific interaction at the adenine N7–C8 locus. Benevides and Thomas,[5] making use of the present NMR results and the coordinates of Zimmerman and Pheiffer,[1] proposed that the observed retardation of C8–H exchange in poly(rA)·poly(dT) is a consequence of close contact of the adenylate 5′ ester oxygen and the adenine C8–H group, resulting in the formation of a stable C8–H···O5′ hydrogen bond. An intranucleotide hydrogen bond of this type would account for the observed retardation of C8–H exchange in poly(rA)·poly(dT) and is consistent with the fiber X-ray data. With the Zimmerman and Pheiffer coordinates,[1] we calculate the H to O distance to be 2.2 Å, which corresponds to a C to O distance of approximately 3.0 Å.[5] The solution structure of $(rA)_8$·$(dT)_8$ proposed here may also suggest a structural basis for understanding the retardation of purine C8–H exchange in other hybrid nucleic acids.

In summary, Raman and NMR spectroscopy indicate a *solution* structure for $(rA)_8$·$(dT)_8$, which is consistent with the *fiber* model proposed for poly(rA)·poly(dT) on the basis of X-ray diffraction.[1] In other applications, structures of this type have been designated by the terms "heteronomous" or "heteromerous".[18,22] The present experimental results imply that such structures may be stabilized in part through the formation of C8–H···O5′ hydrogen bonds within the poly(purine) strand. Intranucleotide C8–H···O5′ hydrogen bonding is also proposed to account for the anomalous hydrogen-exchange characteristics of $(rA)_n$·$(dT)_n$ complexes.[5]

Acknowledgment. This research was supported by Grant AI18758 (G.J.T.) from the U.S. National Institutes of Health, by a grant (Y.K.) from the Ministry of Education, Culture and Science of Japan, and by a Japan–U.S. Cooperative Science Program Grant (Y.K. and G.J.T.) administered jointly by the Japan Society for the Promotion of Science and the U.S. National Science Foundation (INT83-11889). M.K. has been supported in part by a grant for Japanese Junior Scientists from the Japan Society for the Promotion of Science.

Registry No. $(rA)_8$·$(dT)_8$, 126752-58-7.

Supplementary Material Available: The 500-MHz ^1H NMR, the expanded DQF-COSY, and the expanded NOESY spectra of $(rA)_8$·$(dT)_8$ (7 pages). Ordering information is given on any current masthead pages.